

# SPECTROSCOPY AND IMAGING WITH DIFFUSING LIGHT

Visually opaque media are ubiquitous in nature. While some materials are opaque because they strongly absorb visible light, others, such as foam, white paint, biological tissue and milk, are opaque because photons traveling within them are predominantly scattered rather than absorbed. A vanishingly small number of photons travel straight through such substances. Instead, light is transported through these materials in a process similar to heat diffusion (figure 1).

In the physics community there has been substantial recent interest in such diffusing photons. This has led, for example, to the development of dynamic light-scattering probes of turbid complex fluids.<sup>1</sup> In the biophysics and medical communities, diffusing photons are now used to view body function and structure. This is made possible by a spectral window that exists within tissues in the 700–900-nm region, in which photon transport is dominated by scattering rather than absorption (figure 2). Thus, to a very good approximation, near-infrared photons diffuse through human tissue. Two biomedical applications for diffusing near-infrared light probes closely parallel the application of nuclear magnetic resonance to tissue study. Generally, the categories can be termed spectroscopy and imaging. The medical utility of either approach ultimately depends on whether the measured tissue contrast provides enough information to differentiate normal from abnormal body function.

Spectroscopy is useful for the measurement of time-dependent variations in the absorption and scattering of large tissue volumes. For example, brain oxymetry (hemoglobin spectroscopy) of the frontal, parietal or occipital regions can reveal internal bleeding caused by head injury.

Imaging is important when a localized heterogeneity of tissue is involved—for example, an early breast or brain tumor, a small amount of bleeding in the brain or an early aneurysm. Here images enable one to identify the site of the

**Diffusing near-infrared light provides new mechanisms for clinical diagnosis of tissue structure and function.**

Arjun Yodh and Britton Chance

ARJUN YODH is an associate professor of physics and BRITTON CHANCE is a professor emeritus of biochemistry, biophysics and radiology at the University of Pennsylvania, in Philadelphia.

trauma and differentiate it from background tissue.

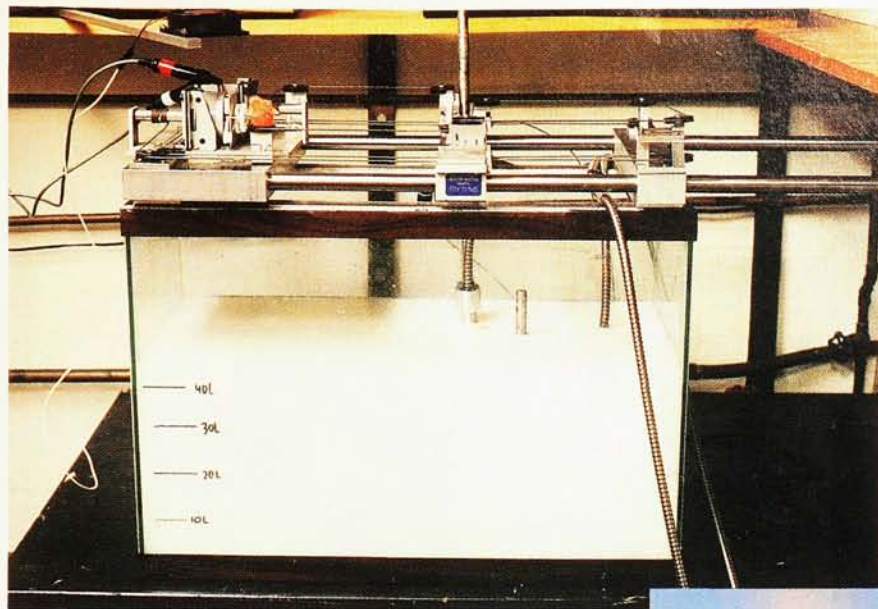
In this article we review the physical basis for tissue characterization in turbid media using diffusing light fields, with examples from our laboratories. We also describe recent clinical applications of the technique. Although the article emphasizes applications, we should note that the roots of the impending clinical impact can be

traced to curiosity-driven research initiated in many small laboratories.

## Diffusive light transport in turbid media

A model of human tissue is shown in figure 1a. Here an aquarium is filled with a milky emulsion called intralipid, whose optical properties in the near-infrared resemble those of tissue. A typical experiment uses one optical fiber to inject near-infrared photons into the medium and a second optical fiber to detect photons at another location. Microscopically, the injected photons experience thousands of elastic scattering events while traveling from one fiber to the other. Occasionally the photons are absorbed in this process and are undetected. The migratory pattern of an individual photon is like a random walk, with each photon trajectory composed of straight line segments and sudden interruptions that randomly change the photon's propagation direction. The length of the straight line segment is often referred to as the transport mean free path, or random-walk step, of the migrating photons.

In our experiments, about  $10^{15}$  photons enter the medium every second. It is impractical to follow individual photon trajectories, so one typically quantifies the light transport problem in terms of more readily measurable macroscopic observables, such as the photon energy density within the sample. This is accomplished by formulating the problem using the diffusion equation. The passage from the random walk to the diffusion equation is well known. We will adopt the diffusion approximation



a

as the starting point of our analysis. Although this central assumption is not always correct,<sup>2</sup> the diffusion approximation for light transport is mathematically simple and has been shown experimentally to be a reasonably good approximation in most of the dense random media, particularly human tissue, with which we are concerned here.

The photon or light energy density  $U(\mathbf{r}, t)$  within the sample is thus assumed to obey the diffusion equation,

$$\nabla \cdot D \nabla U(\mathbf{r}, t) - v \mu_a U(\mathbf{r}, t) - \partial U(\mathbf{r}, t) / \partial t = S(\mathbf{r}, t) \quad (1)$$

Here  $v$  is the speed of light in the medium,  $S(\mathbf{r}, t)$  represents source terms in the medium at position  $\mathbf{r}$  and time  $t$ ,  $D = v[3(\mu_s' + \mu_a)]^{-1}$  is the light diffusion coefficient in the medium,  $\mu_s'$  is the scattering factor of the medium, and  $\mu_a$  is the absorption factor of the medium.

The medium is primarily characterized by two parameters: the scattering factor and the absorption factor. The scattering factor is the multiplicative inverse of the random-walk step length. Its magnitude in tissue is determined in part by the concentration of micron-sized optical heterogeneities, such as cell organelles. The absorption factor depends on the concentration and absorption cross section of various chromophores, such as the hemoglobin that resides in blood vessels. Most generally these quantities will be position and time dependent. Rough estimates of absorption and scattering factors based on recent measurements in living tissues are shown in the table on page 36.

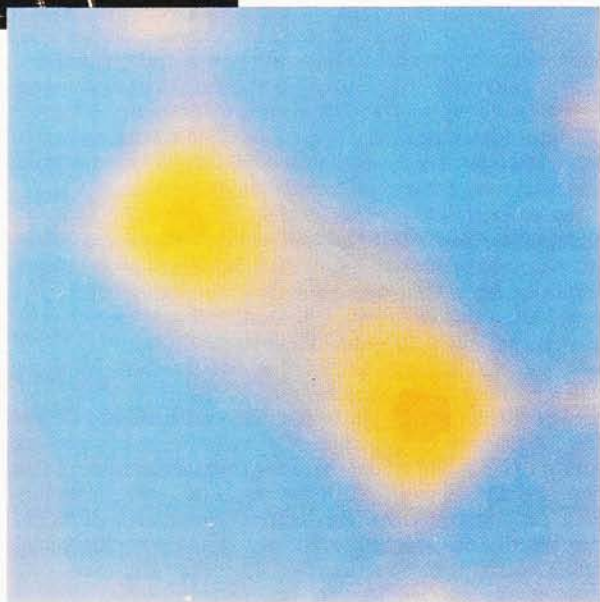
How are the patterns of light energy density distorted as they traverse these media? Early work considered continuous-wave light sources and showed that there was indeed significant information about the medium carried by diffusing light fields in transillumination.<sup>3</sup> More recent experiments and simulations using short-pulse (time-domain),<sup>4,5</sup> amplitude-modulated (frequency domain)<sup>6-10</sup> and continuous-wave<sup>11</sup> sources have sharpened our images and have led to important physical insights and technological innovations.

### Disturbances from cw and modulated light

The elementary disturbances that interest us are generated by point sources of light whose amplitudes are modulated sinusoidally at angular frequency  $\omega$ . In this case the light energy density within the turbid medium can be

### MILKY FLUID AND IMAGE OF EMBEDDED OBJECTS.

a: Aquarium used for model experiments is filled with intralipid, an emulsion whose absorption and scattering in the near-infrared can be adjusted to approximate those of tissue.  
b: Slice of a reconstructed image of two heterogeneities: 1-cm-diameter absorbing spheres embedded in the emulsion. Source-detector separations were 6 cm. Image reconstruction was based on equation 3. (From ref. 14.)  
FIGURE 1



b

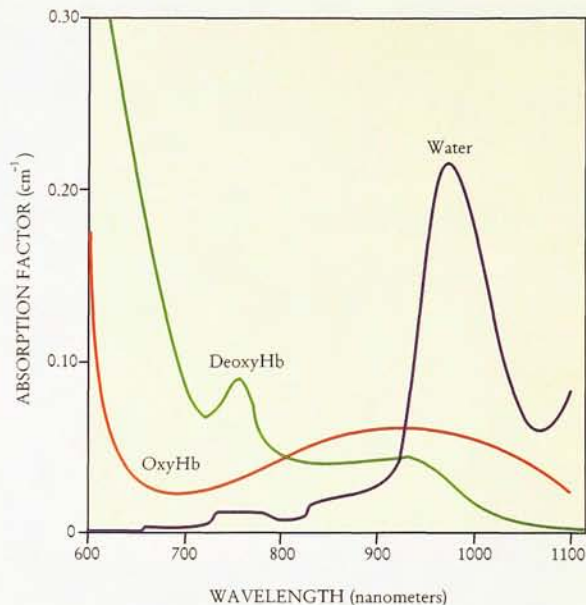
written as a sum of time-independent and time-dependent parts:  $U(\mathbf{r}) = U_{dc}(\mathbf{r}) + U_{ac}(\mathbf{r}) \exp(-i\omega t)$ . We will be concerned mainly with the time-dependent solutions. Disturbances from continuous-wave sources can be derived, apart from multiplicative changes in amplitude, from the time-dependent solutions by setting  $\omega$  to zero. In the presence of an oscillating point source at the origin, it is straightforward to show that the spatial part of the time-dependent solution at frequency  $\omega$  obeys the Helmholtz equation,

$$[\nabla^2 + k^2]U_{ac}(\mathbf{r}) = \delta(\mathbf{r})A/D \quad (2)$$

with  $k^2 = (-v\mu_a + i\omega)/D$ . Here  $A$  represents the product of the source modulation and strength, and the medium is assumed to be homogeneous. If the medium is infinite, then the solution to equation 2 is a highly damped, spherical wave. Microscopically, individual photons undergo a random walk within the medium, but collectively, a spherical wave of photon density is produced and propagates outward from the source. Hereafter we refer to this disturbance as a diffuse photon-density wave.

In the absence of absorption, the real and imaginary

*IN VITRO* ABSORPTION SPECTRA of hemoglobin and water, showing a spectral window in tissue in the near-infrared. The window is brought about by a decrease in blood (oxy- and deoxyhemoglobin) absorption and an increase in water absorption. The concentrations of hemoglobin and water were adjusted to approximate values found in tissue such as the brain. These data were taken recently by Konda Reddy at the University of Pennsylvania. Absorptions are reported as natural logarithms. FIGURE 2



parts of the wavevector  $k$  are equal, and the wavelength is effectively the root-mean-square displacement experienced by a typical photon during a single modulation period. When the effects of absorption are included, the wavelength decreases, and the real and imaginary parts of the wavevector are no longer equal. Although the wave attenuates very rapidly, it has a well-defined wavelength, amplitude and phase at all points. This type of disturbance, which was first reported in the biophysics community by Enrico Gratton and his coworkers at the University of Illinois, Urbana-Champaign,<sup>6</sup> arises formally in any diffusive system driven by an oscillating source.<sup>12</sup>

There are a variety of ways to generate diffuse photon-density waves.<sup>6-10</sup> Typically, amplitude-modulated light is delivered into the turbid sample through a source fiber-optic cable, and the scattered photons are collected through a detector fiber-optic cable. The source radiation is derived from a light-emitting diode, diode laser or more complex laser system. The oscillating portion of the detected diffuse light energy density is separated from all other light by standard phase-sensitive methods. Both the phase and amplitude of the diffuse photon-density wave can be determined in this way. In figure 3a the measured wave is demonstrated within a tank of homogeneous intralipid.<sup>8</sup> Constant-phase contours are shown in 20° intervals about the source at the origin. We see that the wave contours are circular and that their radii can be extrapolated back to the source. In figure 3b the phase shift and a function of the wave amplitude are plotted against the radial distance from the source. From these position-dependent measurements, one can deduce the wavelength of the disturbance (11 cm), as well as the absorption and scattering factors of the homogeneous turbid medium.

## Interaction of light and tissue

Tissue	Scattering factor $\mu_s'(\text{cm}^{-1})$	Absorption factor $\mu_a(\text{cm}^{-1})$	Number of samples
Human brain (820 nm)	17.5 ( $\pm 1$ )	0.04 ( $\pm 0.01$ )	33
Human breast (780 nm)	15 ( $\pm 2.3$ )	0.035 ( $\pm 0.01$ )	700
Rat brain (780 nm)	13.2 ( $\pm 0.8$ )	0.15 ( $\pm 0.02$ )	3
Rat white adipose tissue (780 nm)	18.6 ( $\pm 1.4$ )	0.07 ( $\pm 0.01$ )	5

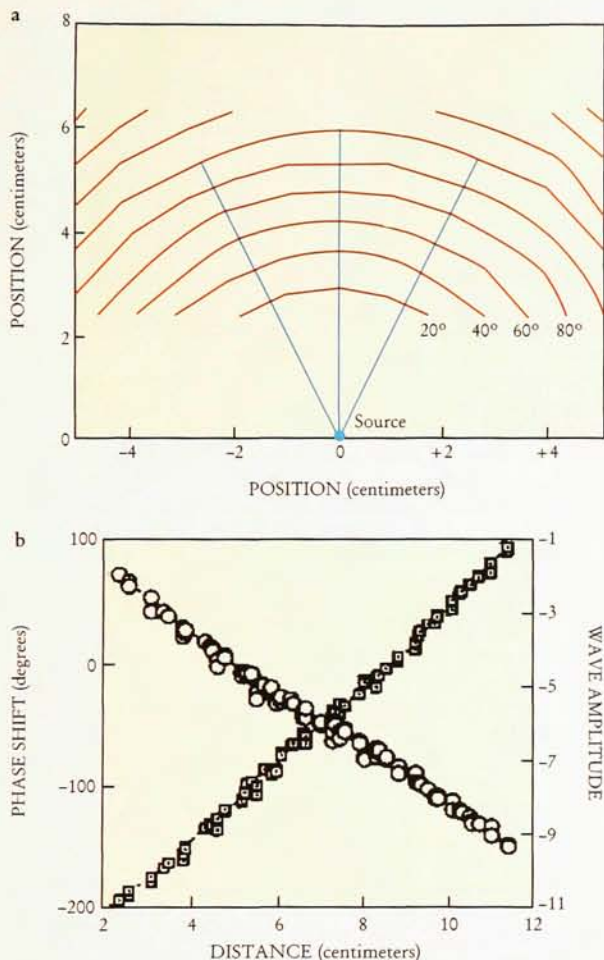
Human brain data are from reference 24. Human breast data are from S. Nioka, University of Pennsylvania. Rat-tissue data are from ref. 16. The measurements employ pulse-time methods, with simplified fitting functions based on homogeneous semi-infinite turbid media.

Although these waves are overdamped, it is feasible to use them as probes of biological samples measuring on the order of 10 cm, or about 100 transport mean free path lengths. The measurements will necessarily be in the near field of the diffuse photon-density wave, but analogies from optics often help one to understand the variation of the amplitude and phase of the diffuse photon-density waves brought about by absorption and scattering changes within the sample.

Figure 4 shows the scattering of a diffuse photon-density wave by a spherical obstacle located within an otherwise turbid homogeneous medium.<sup>9,13</sup> This is a model for a simple imaging measurement where the diffuse photon-density waves are used to resolve the variation in the absorption factor of discrete volumes within heterogeneous tissues. The problem is very similar to Mie scattering in optics and can be understood in detail in terms of a partial wave analysis.<sup>13</sup> Variations in the phase and amplitude contours of the scattered wave can be easily used to deduce information about the position, size, absorption and scattering of the discrete spherical object.

The diffusive waves have been observed to exhibit other properties one normally associates with conventional electromagnetic radiation, such as refraction,<sup>8</sup> diffraction,<sup>6,9</sup> interference<sup>7</sup> and dispersion.<sup>10</sup> Contrast in these cases is brought about by variations in absorption and scattering, which combine to produce effective dielectric constants for the diffusive waves. For example, the dispersion of the wave's phase and modulation ( $|U_{ac}|/|U_{dc}|$ ) as a function of frequency  $\omega$  provides sufficient information to characterize time-dependent changes of average absorption and scattering in bulk tissue.<sup>10</sup>

Thus far our discussion has centered on the production and use of single-frequency diffuse photon-density waves. There exist, however, a variety of experimental approaches for probing turbid media with diffusing near-infrared light. A particularly simple approach uses continuous-wave sources.<sup>3,11</sup> In this case the diffusing light energy density has a purely imaginary wavevector that depends solely on the absorption and scattering factors of the medium. The distortion of constant-amplitude contours provides information about the sample, but because the disturbance does not oscillate in time, phase informa-



MEASURED PHOTON-DENSITY WAVE phase and amplitude. **a:** Constant-phase contours of diffuse photon-density wave in a homogeneous sample of intralipid. The source for this measurement is a 1-mW laser diode operating at 780 nm and modulated at 200 MHz. **b:** Measured phase (squares) and a dimensionless logarithmic function of the amplitude and source-detector separation (circles) plotted as a function of distance from the source. (From ref. 8.) FIGURE 3

It is not clear which experimental approach will ultimately find the most use in medicine. For a single source-detector pair, the pulsed-time approach clearly carries more information, as a result of the many components of its diffuse photon-density waves. However, modulated optical systems that employ several well-chosen, discrete frequencies or that use continuous frequency variation may be technically simpler, while providing the same essential information needed by physicians.

### Functional imaging and object localization

Near-infrared diffusing light probes offer new techniques for clinical diagnosis of the human body's structure and function. Optical contrast can result from changes in tissue blood volume and blood oxygenation. Such changes affect the wavelength-dependent absorption factor of the tissue volume. In addition, one can induce absorption variation within tissue by administering chemicals that preferentially accumulate in diseased tissue. Such contrast agents are used in positron emission tomography and sometimes in magnetic resonance imaging. Variation of the scattering factor affords a novel source of contrast that is demonstrably affected by intracellular organelles such as mitochondria.<sup>16</sup> It also depends on the fat, water and perhaps even glucose concentration in tissue.<sup>17</sup>

The spectrum of biophysical problems that are currently being pursued with these instruments ranges from studies of oxygen dynamics in the brain to the identification of internal bleeding to the detection of structural anomalies such as tumors. Brain studies are promising because light in the near-infrared penetrates the skull much more effectively than does, for example, ultrasound. Measurements of oxygen dynamics are facilitated because optical spectra are intrinsically sensitive to blood oxygenation; mri, by comparison, detects blood indirectly. In addition, the nature of medical optical imaging favors the widespread use of diffusing light probes, because the instruments are compact, portable and inexpensive and rely only upon electro-optical components that are small and efficient, such as laser diodes and miniature photomultiplier tubes.

Figure 5a, which shows blood that has accumulated from bleeding in the front of an adult brain,<sup>18</sup> demonstrates the utility of spectroscopy. Here the escaping blood greatly exceeds in volume the ruptured vessels from which it leaks and gives a very distinctive contrast as a result of hemoglobin absorption in a localized region of the brain. The diffusing photons penetrate the skin, skull and dura, and are absorbed asymmetrically by the afflicted and normal sides of the brain.

Figure 5b illustrates a second example. This graph is a record of the changes in blood oxygen saturation in the brain of a nine-month-old baby undergoing cardiopulmonary bypass surgery.<sup>19</sup> In these measurements, low-frequency (or continuous wave) photon sources at multiple wavelengths (760 nm and 800 nm) are used alternately. The wavelength dependence of the tissue scattering factor is small, but the wavelength-dependent blood absorption is large, and ratiometric schemes can be easily employed to estimate relative changes in oxygen saturation.<sup>20</sup>

tion is not available.

*A priori* one might expect the sensitivity with modulated disturbances to be greater than that with continuous-wave sources. In tissue, however, when the background absorption factor is large (greater than, say,  $1.0 \text{ cm}^{-1}$ ), images of absorptive heterogeneities are not significantly improved at higher modulation frequencies (for example, 1 GHz). Generally, image quality can be improved at higher frequency only when the modulation frequencies exceed the photon absorption rate ( $\nu\mu_a$ ) within the turbid medium.<sup>14</sup> Thus one of the advantages of using modulated sources to detect absorptive inhomogeneities is partially offset in human subjects as a result of relatively high photon absorption rates.

A third experimental approach uses mode-locked trains of short light pulses.<sup>4</sup> The pulsed-time methods—which should be distinguished from time-domain techniques using only unscattered, or “ballistic,” photons<sup>15</sup>—derive their information about the sample from changes in the temporal shape of the photon pulse that occur as the pulse traverses the medium. Loosely speaking, the peak time delay of the broadened pulse depends on the scattering factor, and the terminal slope depends on the sample absorption factor. Formally, one can treat the pulse trains as a superposition of diffuse photon-density waves with different modulation frequencies. The transport and scattering of the pulses can thus be viewed in terms of a superposition of diffuse photon-density waves, each of which scatters independently. Analysis of the broadened pulse trains can proceed via time- or frequency-domain techniques.

Among other things, this type of information is useful in determining which heart treatments are the most dangerous to the brain during surgery.

Because tissue is often quite heterogeneous, it is natural to contemplate making images with the diffusive waves. Resolutions comparable to those of PET and MRI (several millimeters) are highly desirable, but a range of problems exists for which resolutions of about 1 cm are useful. A simple example of the utility of imaging is the early localization of a head injury that causes brain bleeding or hematomas. Here continuous-wave light devices can detect minor bleeding in the brain<sup>18</sup> that is at the limit of detection using x-ray computed tomography. Such sensitivities in detecting hematomas suggest it may be possible to localize small blood vessel expansions (aneurysms), which must be detected at levels below 1 cm if rupture of the vessel is to be avoided. (See the article by George Hademenos in *PHYSICS TODAY*, February, page 24.)

Tumors are another type of structural anomaly that one wants to detect, localize and classify. One common property of rapidly growing tumors—a property that has been exploited by a whole subfield of MRI—is the leakiness of their blood vessels. These blood vessels will leak paramagnetic contrast agents (small molecules) at a greater rate into the tumor space than into the adjacent normal tissue. The optical method can observe the tagging of small tumors by an optical contrast agent, for example, indocyanine green. In the long term it may be possible to design contrast agents that respond to specific properties of tumors, such as their membrane potential or their organelles. The optical method, however, can look at other properties associated with tumor growth: larger blood volume resulting from a larger number density and volume fraction of blood vessels residing within the tumor, blood deoxygenation arising from relatively high metabolic activity within the tumor, increased concentrations of the intracellular organelles necessary for the energy production associated with rapid growth, and the accumulation of highly scattering calcium precipitates. Some of these properties may prove particularly helpful in classifying tumors as benign, malignant and so on.

There are many other types of tissue that can be studied, including the neonatal brain and lungs, and the human breast. The new tools may make possible a range of physiological studies of hemodynamics in relation to the oxygen demand of various body organs. Perhaps most important is the change of oxygen delivery that occurs in the functional brain, especially during mental activity.<sup>21</sup>

## Recent progress in imaging

The majority of imaging experiments have been carried out using model systems similar to the intralipid setup

shown in figure 1. Such experiments are useful because they enable one to delineate clearly the theoretical limits of the techniques and to develop the technology further. Our discussion will center on these model experiments.

The central issues to be considered are: How small an object can be detected and localized? And how accurately can objects be characterized? The answers depend on many factors, including absorption contrast with respect to the background medium, uncertainty in the positioning of sources and detectors, shot noise (fluctuations due to the discrete nature of the signal being measured), boundaries, the source modulation frequency and the sensitivity to noise of inversion algorithms. We will give a synopsis of these issues and describe some of the imaging methods currently employed. However, because the technologies and approaches are rapidly evolving, we will not provide "golden" limits.

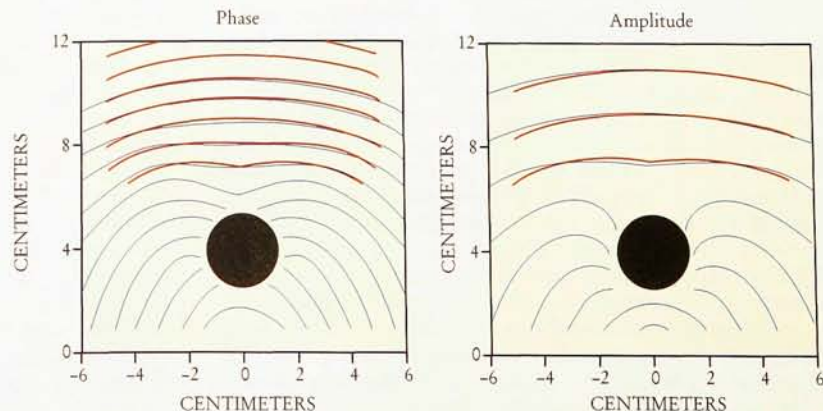
A number of general answers can be gleaned from experiments of the type shown in figure 4, where a single spherical object is embedded in a uniform and essentially infinite background medium. The first question we consider in this very ideal situation is whether one can detect the existence of the spherical object for practical source-detector separations and signal-to-noise ratios. One can easily show that the amplitude change induced by a 3-mm-diameter absorber with an absorption factor four times as large as a background absorption  $\mu_a$  of 0.4/cm is about 3% of the unperturbed amplitude measured 8 cm from the source, directly behind the object. Although the object scatters light weakly, the differential change in signal is large in comparison with a conservative shot-noise detection floor of  $10^{-4}$  during a 1-second time interval. Detection of objects in the submillimeter range is possible under these ideal circumstances.

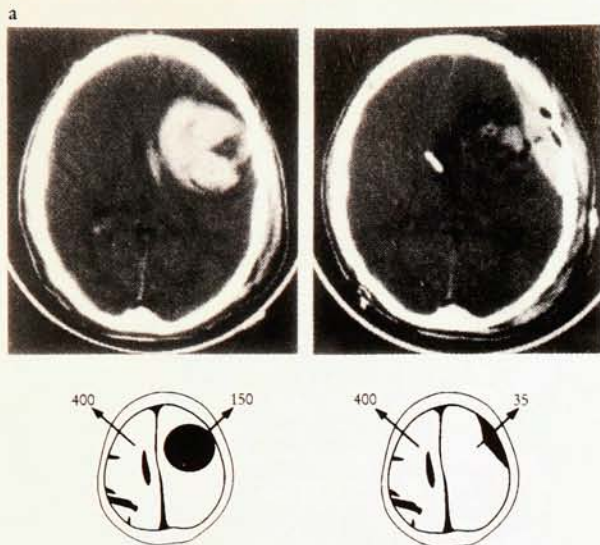
While useful for some diagnostic procedures, object detection is not object localization: One wants to determine the position, size, shape and optical properties of the heterogeneity. Simple object-positioning devices have been constructed that use the interference (or comparison) of signals at detector positions equidistant from two spatially separated sources.<sup>7</sup> In the absence of heterogeneities the signals will cancel, but large changes in phase and amplitude are observed when a small object crosses the "line of sight" of the source-detector pair. In sufficiently homogeneous media, this type of "pointing" device can be used to estimate the position of a very small (say, 50 mg in mass, containing 100 picomoles of absorber) single irregularity to an accuracy of better than 1 mm. Thus fine localization of single objects appears feasible with continuous and modulated source arrays, which can operate in digital or analog modes.

Complete information about object shapes and optical

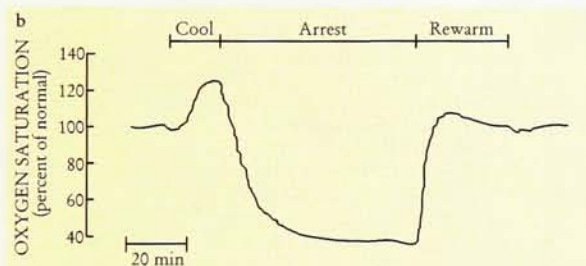
SCATTERING of a diffuse photon-density wave by a perfectly absorbing spherical obstacle 2.6 cm in diameter. Red lines are experimental contours of constant phase and amplitude. Blue lines represent theoretical predictions based on partial wave expansion. (See refs. 9 and 13.)

FIGURE 4





SPECTROSCOPY OF BLOOD. a: X-ray computed tomography images of a hematoma in a patient's brain before (left) and after (right) surgical removal of blood. In both cases blood leakage on the right side of the brain is observed. The diagrams below the images show the scheme for the visible-light spectroscopy measurements. In each case, light reflected in the hematoma side of the brain was compared with that reflected in the normal side. The differential spectroscopy measurements clearly indicated the asymmetry in blood volume and, importantly, the reoccurrence of bleeding after the operation. The numbers represent light intensities; notice that the optical method is much more sensitive to the epidural (shallow) bleeding on the right than to the cranial (deep) bleeding on the left. (From ref. 15.) b: The dynamics of blood oxygen saturation in a nine-month-old baby during cardiopulmonary bypass surgery. We see how the base-line saturation at the start of the operation increases with cooling just before arrest. During arrest the saturation decreases and stabilizes. It returns to normal after the patient is warmed. (Adapted from ref. 19.) FIGURE 5



properties in heterogeneous media requires tomographic approaches to data acquisition and inversion. The last few years have seen extensive work along these lines.<sup>3,5,14,22</sup> The problem in essence amounts to inverting equation 1. This is more complicated than the computerized tomography approach, because the photons do not travel in straight lines through the sample.

Suppose we have a tissue sample with relatively large fractional changes in the absorption factor but small average variations in the scattering factor. Under these circumstances one can solve the problem perturbatively in the absorption variation. The lowest-order deviation  $\Delta U$  between the detected light energy density and the light energy density that would have been detected in a uniform background can be written in the form

$$\Delta U(\mathbf{r}_s, \mathbf{r}_d) = - \int G(\mathbf{r}, \mathbf{r}_d) [v \Delta \mu_a(\mathbf{r}) / D] U_o(\mathbf{r}, \mathbf{r}_s) d^3 \mathbf{r} \quad (3)$$

Here  $\mathbf{r}_d$  and  $\mathbf{r}_s$  are the detector and source positions, respectively,  $\mathbf{r}$  is a position in the sample,  $G(\mathbf{r}, \mathbf{r}_d)$  is the Green's function solution to equation 2 in the appropriate geometry,  $\Delta \mu_a(\mathbf{r})$  is the position-dependent change in absorption factor with respect to the background absorption, and  $U_o(\mathbf{r}, \mathbf{r}_s)$  is the disturbance at position  $\mathbf{r}$  due to a source at position  $\mathbf{r}_s$  in the absence of perturbations. Equation 3 is a Born perturbation expansion. Other expansions, such as the Rytov expansion, can be used with equation 1 to generate solutions that are valid in higher orders under qualitatively different physical conditions.<sup>23</sup>

One solves equation 3 numerically by making the equation discrete on a grid. Such an approach yields a set of linear equations relating measurements of the disturbance over a range of source and detector positions to the value of the absorption change at specific volume elements within the sample. There are then many direct

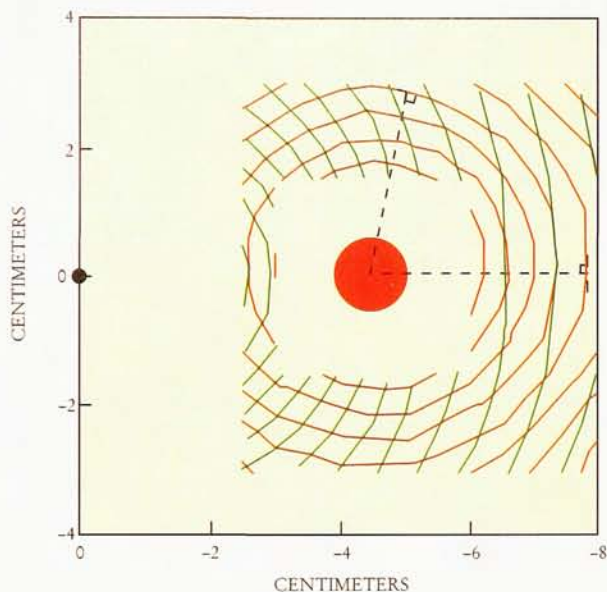
and indirect methods to find solutions to the inverse problem, although it should be noted that the problem is ill posed and is sensitive to measurement noise.<sup>23</sup> Figure 1 shows an example of such a reconstruction using equation 3. Measurements were made in the aquarium of figure 1, so that the geometry could be considered infinite and homogeneous except for two discrete absorptive inhomogeneities placed in the sample.<sup>14</sup>

These techniques are general but require extensive computer memory and time, particularly as the smallest volume element is reduced in size. Typical reconstructions using these more general techniques can distinguish structures of approximately 1 cm in size; sharp edges are typically blurred by a few millimeters. This is adequate for many functional imaging applications. The problem becomes somewhat more complicated and more sensitive to noise when variations in the scattering factor are included.

As a final imaging example we consider the use of optical contrast agents. Figure 6 illustrates the basic effect underlying this methodology.<sup>7,9</sup> Here the reemission of a diffuse photon-density wave by a fluorescent obstacle was accomplished by filling a spherical glass shell with the dye indocyanine green and then illuminating the sphere with a diffuse photon-density wave in the intralipid solution. The dye absorbs radiation at the source wavelength of 780 nm, and about a nanosecond later it reradiates photons at a redshifted energy of 830 nm. In figure 6 the measured constant-amplitude contours of the incident wave at 780 nm appear as green lines and those of the secondary wave at 830 nm as red lines. The diffuse photon-density wave character of the reradiated waves is clearly revealed. We see that the reradiated wave originates from within the absorbing obstacle. In the process, the inhomogeneity is converted into a source of secondary diffuse photon-density waves with reduced background. This process is applicable in tissue that selectively retains contrast agents.

## Outlook

We have described some novel applications of simple optical principles to diffusive waves propagated in highly scattering media that simulate the scattering and absorption properties of human tissue. While computer simulations and model experimental studies verify the high functional sensitivity of these methods, they are approximate and are inadequate for the full treatment of real



REEMISSION of a diffuse photon-density wave by a fluorescent obstacle. The diagram shows measured constant-amplitude contours of incident (green lines) and reradiated (red lines) diffuse photon-density waves around a spherical shell containing indocyanine green dye and intralipid. The point at the origin represents the source of the incident waves. The measurements were obtained in the aquarium of figure 1. (See ref. 9.) FIGURE 6

tissue, where boundary conditions, multiple heterogeneities and limitations of the diffusion approximation are evident. Nevertheless, early studies of these techniques in human tissue have been encouraging. Continuing improvement in the sensitivity, speed, size and efficiency of related technologies will further enhance these novel approaches to clinical studies of tissue function in normal and pathological states.

We thank our colleagues worldwide for many illuminating discussions over the last few years. We particularly wish to acknowledge collaborations and discussions with scientists at the University of Pennsylvania, including Bertran Beauvoit, David Boas, Michael Cohen, Jack Leigh, Dean Kurth, Hanli Liu, Tom Lubensky, Shoko Nioka, Maureen O'Leary and John Schotland. Our work is supported by the National Science Foundation (Yodh) and the National Institutes of Health (Chance).

## References

1. G. Maret, P. E. Wolf, *Z. Phys. B* **65**, 409 (1987). M. J. Stephen, *Phys. Rev. B* **37**, 1 (1988). D. J. Pine, D. A. Weitz, P. M. Chaikin, E. Herbolzheimer, *Phys. Rev. Lett.* **60**, 1134 (1988).
2. See, for example, A. Ishimaru, *Wave Propagation and Scattering in Random Media*, Academic, New York (1978). S. Glasstone, M. C. Edlund, *The Elements of Nuclear Reactor Theory*, Van Nostrand, New York (1952), chs. 5, 14. K. M. Case, P. F. Zweifel, *Linear Transport Theory*, Addison-Wesley, Reading, Mass. (1967), ch. 8 and references therein.
3. J. R. Singer, F. A. Grunbaum, P. Kohn, J. Zubelli, *Science* **248**, 990 (1990). F. F. Jobsis, *Science* **198**, 1264 (1977). For many examples of continuous-wave imaging with diffuse light, see work in the field of diaphanography: M. Kaneko *et al.*, *Radiat. Medicine* **6**, 61 (1988) and references therein.
4. M. S. Patterson, B. Chance, B. C. Wilson, *Appl. Opt.* **28**, 2331 (1989). B. Chance *et al.*, *Proc. Natl. Acad. Sci. USA* **85**, 4971 (1988). D. T. Delpy, M. Cope, P. van de Zee, S. Arridge, S. Wray, J. Wyatt, *Phys. Med. Biol.* **33**, 1433 (1988). S. L. Jacques, *Appl. Opt.* **28**, 2223 (1989). D. A. Benaron, D. K. Stevenson, *Science* **259**, 1463 (1993).
5. J. Chang, Y. Wang, R. Aronson, H. L. Graber, R. L. Barbour, in *Proc. Inverse Problems in Scattering and Imaging*, M. A. Fiddy, ed., SPIE, Bellingham, Wash. (1992), p. 384.
6. E. Gratton, W. Mantulin, M. J. van de Ven, J. Fishkin, M. Maris, B. Chance, in *Proc. 3rd Int. Conf. Peace Through Mind/Brain Science*, Y. Yamashita, ed., Hamamatsu Photonics, Hamamatsu, Japan (1990), p. 183. J. Fishkin, E. Gratton, *J. Opt. Soc. Am. A* **10**, 127 (1993).
7. J. M. Schmitt, A. Knüttel, J. R. Knutson, *J. Opt. Soc. Am. A* **9**, 1832 (1992). A. Knüttel, J. M. Schmitt, J. R. Knutson, *Appl. Opt.* **32**, 381 (1993). A. Knüttel, J. M. Schmitt, R. Barnes, J. R. Knutson, *Rev. Sci. Instrum.* **46**, 638 (1993).
8. M. A. O'Leary, D. A. Boas, B. Chance, A. G. Yodh, *Phys. Rev. Lett.* **69**, 2658 (1992).
9. D. A. Boas, M. A. O'Leary, B. Chance, A. G. Yodh, *Phys. Rev. E* **47**, R2999 (1993). M. A. O'Leary, D. A. Boas, B. Chance, A. G. Yodh, *J. Lumin.* **60-61**, 281 (1994).
10. B. J. Tromberg, L. O. Svaasand, T. T. Tsay, R. C. Haskell, *Appl. Opt.* **32**, 607 (1993). E. M. Sevick, J. Lakowicz, H. Szmajnski, K. Nowaczyk, M. L. Johnson, *J. Photochem. Photobiol. B* **16**, 169 (1992).
11. M. Takada, T. Tamura, M. Tamura, *Adv. Exp. Med. Biol.* **215**, 301 (1987). H. L. Graber, J. Chang, J. Lubowsky, R. Aronson, R. L. Barbour, in *Proc. Photon Migration and Imaging in Random Media and Tissues*, B. Chance, R. Alfano, eds., SPIE, Bellingham, Wash. (1993), p. 372. M. Kashke, H. Jess, G. Gaida, J.-M. Kaltenbach, W. Wrobel, in *Proc. Advances in Optical Imaging and Photon Migration*, R. R. Alfano, ed., Opt. Soc. Am., Washington, D.C. (1994), p. 88.
12. H. S. Carslaw, J. C. Jaeger, *Conduction of Heat in Solids*, Oxford U. P., Oxford, England (1959).
13. D. A. Boas, M. A. O'Leary, B. Chance, A. G. Yodh, *Proc. Natl. Acad. Sci. USA* **91**, 4887 (1994). For similar calculations and measurements for small objects and continuous sources, see P. N. den Outer, Th. M. Nieuwenhuizen, A. Lagendijk, *J. Opt. Soc. Am. A* **10**, 1209 (1993).
14. M. A. O'Leary, D. A. Boas, B. Chance, A. G. Yodh, *Opt. Lett.* **20**, 426 (1995).
15. L. Wang, P. P. Ho, C. Liu, G. Zhang, R. R. Alfano, *Science* **253**, 769 (1991).
16. B. Beauvoit, H. Liu, K. Kang, P. D. Kaplan, M. Miwa, B. Chance, *Cell Biophys.* **23**, 91 (1993). B. Beauvoit, S. M. Evans, T. Jenkins, E. Miller, B. Chance, to be published in *Anal. Biochem.*
17. M. Kohl, M. Essenpries, D. Booker, M. Cope, in *Proc. Conf. Optical Tomography, Photon Migration, and Spectroscopy of Tissue and Model Media: Theory, Human Studies, and Instrumentation*, B. Chance, R. Alfano, eds., SPIE, Bellingham, Wash. (1995).
18. S. P. Gopinath, C. S. Robertson, R. G. Grossman, B. Chance, *J. Neurosurg.* **79**, 43 (1993).
19. C. D. Kurth, J. M. Steven, S. C. Nicolson, *Anesthesiology* **82**, 74 (1995).
20. D. T. Delpy, S. R. Arridge, M. Cope, *Adv. Exp. Med. Biol.* **248**, 41 (1989). E. M. Sevick, B. Chance, J. Leigh, S. Nioka, M. Maris, *Anal. Biochem.* **195**, 330 (1991).
21. B. Chance, Z. Zhuang, C. Unah, C. Alter, L. Lipton, *Proc. Natl. Acad. Sci. USA* **90**, 3770 (1993).
22. S. R. Arridge, in *Medical Optical Tomography: Functional Imaging and Monitoring*, G. Muller, ed., SPIE, Bellingham, Wash. (1993), p. 31. S. R. Arridge, P. van de Zee, M. Cope, D. T. Delpy, in *Proc. Time-Resolved Spectroscopy and Imaging of Tissues*, B. Chance, ed., SPIE, Bellingham, Wash. (1991), p. 204. M. A. O'Leary, D. A. Boas, B. Chance, A. G. Yodh, in *Proc. Advances in Optical Imaging and Photon Migration*, R. R. Alfano, ed., Opt. Soc. Am., Washington, D.C. (1994), p. 106. J. C. Schotland, J. C. Haselgrove, J. S. Leigh, *Appl. Opt.* **32**, 448 (1993).
23. A. C. Kak, M. Slaney, *Principles of Computerized Tomographic Imaging*, IEEE, New York (1988).
24. D. S. Smith, W. J. Levy, S. Carter, M. Haida, B. Chance, in *Proc. Photon Migration and Imaging in Random Media and Tissues*, B. Chance, R. Alfano, eds., SPIE, Bellingham, Wash. (1993), p. 511. ■